ACS Partner Journal

ACCOUNTS of materials research

pubs.acs.org/amrcda

Article

Multibranched-Based Fluorinated Materials: Tailor-Made Design of ^{19}F-MRI Probes

Beatrice Lucia Bona, Olga Koshkina, Cristina Chirizzi, Valentina Dichiarante, Pierangelo Metrangolo,* and Francesca Baldelli Bombelli*

Cite This: https://doi.org/10.1021/accountsmr.2c00203

Read Online

ACCESS | Metrics & More | Article Recommendations

CONSPECTUS: Future medicine is primarily aiming at the development of novel approaches for an early diagnosis of diseases and a personalized therapy for patients. For achieving these objectives, a key role is played by medical imaging. Among available noninvasive imaging techniques, Fluorine-19 (^{19}F) Magnetic Resonance Imaging (MRI) is emerging as a powerful quantitative detection modality for clinical use both for molecular imaging and for cell tracking. The strength of using ^{19}F-MRI is mainly related to the lack of endogenous organic fluorine in tissues, with no background, enabling the visualization of fluorinated tracers as *hot-spot* images, adding secondary independent information to the anatomical features provided by the grayscale ^{1}H-MRI. The main challenge for ^{19}F-MRI clinical application is the intrinsic reduced sensitivity of MRI. To improve sensitivity, undoubtedly the use of a high field MRI scanner and cryogenic radiofrequency probes is advantageous, but there is a clear need of developing increasingly effective fluorinated tracers.

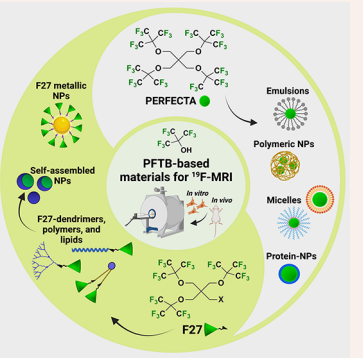

The ideal tracer should bear as many as possible magnetically equivalent fluorine atoms and show optimal magnetic resonance relaxivity properties (i.e., T_1 and T_2), which enable reduced acquisition time with the possibility to apply fast imaging methods. Moreover, it should be biocompatible with reduced tendency to bioaccumulate in tissues, which is one of the main drawbacks in using perfluorocarbons (PFCs), together with their difficulty to be chemically modified with functional groups. In fact, PFCs such as perfluorooctyl bromide (PFOB), perfluoro-15-crown-5-ether (PFCE), and linear perfluoropolyethers (PFPE) are currently the most used tracers in ^{19}F-MRI preclinical and clinical studies, with the above-mentioned limitations. In this regard, molecules bearing short branched fluorinated chains gained a lot of attention for their high number of equivalent fluorines and expected capability of reducing bioaccumulation concerns. A valuable building block for branched fluorinated tracers is perfluoro-*tert*-butanol (PFTB), with nine magnetically equivalent fluorines and easy availability and modification.

In this Account we will discuss the main challenges that ^{19}F-MRI has to overcome for increasing its clinical use, highlighting on one hand the need of developing customized fluorinated materials for increasing sensitivity and enabling multimodal properties, and on the other hand, the importance of the ultrastructure of the final formulation for the final biological response (i.e., clearance). In this context, our group has been focusing on the synthesis and development of branched fluorinated tracers, for which the *originator* is a molecule called PERFECTA (from suPERFluorinatEdContrasT Agent), bearing 36 equiv ^{19}F atoms, which showed not only optimal relaxometry properties but also a very specific and intense Raman signal. Thus, PERFECTA and its derivatives represent a new family of multimodal tracers enabling multiscale analysis, from whole body imaging (^{19}F-MRI) to microscopic detection at the cellular/tissue level (Raman microscopy). We believe that our proposed PFTB strategy can strongly promote the production of increasingly effective ^{19}F-MRI materials with additional functionalities, facilitating the clinical translation of this imaging modality.

1. INTRODUCTION

Magnetic Resonance Imaging (MRI) is an ideal technique in biology and medicine, as it allows researchers to simultaneously visualize anatomical structures and obtain specific molecular information, as well. Hydrogen (^{1}H) nuclei in body water are the best target for *in vivo* MRI because, among all types of nuclei in the body, they provide the highest nuclear MR signal and achieve good contrast between different tissues. However, ^{1}H-MRI sensitivity issues require the administration of high concentrations of contrast agents (CA), possibly causing toxicity concerns, as recently emerged for gadolinium (Gd^{3+})-based ones.[1] Moreover, the urgent need to localize complex molecular activities *in vivo*, as well as track and quantify targets of biological interest (i.e., drugs, nanoparticles, etc.), determined the fast development of heteronuclear

Received: October 14, 2022
Revised: December 16, 2022

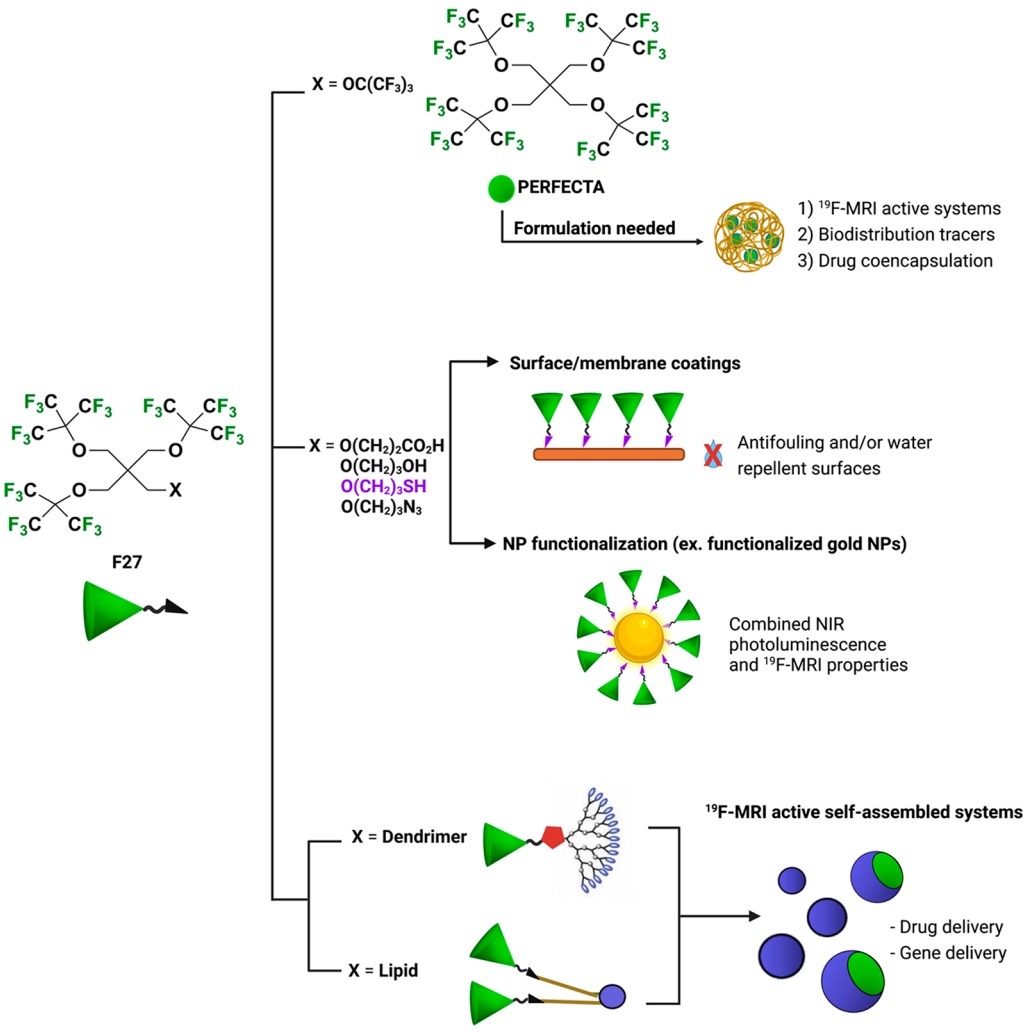

Figure 1. Schematic representation of PERFECTA-based partially fluorinated macromolecules and derivatives and their possible applications.

fluorine, sodium, phosphorus, and other tracers and imaging technologies.[2]

The ^{19}F nucleus with its 100% natural abundance, high gyromagnetic ratio (40.06 MHz/T), wide range of chemical shift (<350 ppm), and 83% sensitivity of ^{1}H is considered one of the most promising imaging nuclei. Thus, ^{19}F-MRI emerged as an extremely powerful quantification and tracking technique providing complementary information to ^{1}H-MRI.[3] Due to the lack of detectable endogenous fluorine in the human body (only present as inorganic fluorine in bones and teeth),[4] ^{19}F-MRI does not suffer of any background signals (signals derive only from the fluorine atoms contained in the used fluorinated tracer), allowing for "hot-spot" images that add secondary independent information (i.e., biodistribution) in addition to the anatomical features provided by the anatomical/morphological ^{1}H-MRI. The absence of a proper background signal of ^{19}F-MRI is a strong feature that makes this technique suitable for unbiased localization and tracking of fluorinated probes over time, contrary to what is observed for other ^{1}H-based standard CAs. For example, superparamagnetic iron oxide nanoparticles (SPIONs) are characterized by poor specificity due to the absence of MRI signal linearity with CA concentration, thus preventing a quantitative and accurate analysis.[5,6]

Since SPIONs detection is unspecific, they can be confused with the endogenous iron present in healthy and diseased tissues (hemorrhage or necrosis). Moreover, their presence could strongly alter MRI signals from protons (^{1}H), thus interfering with standard imaging analysis.

However, besides all the just discussed strengths, ^{19}F-MRI clinical application is still a challenge mainly due to the reduced intrinsic sensitivity of MRI, stimulating the search of increasingly effective fluorinated tracers. An ideal ^{19}F-MRI tracer should contain a high number of equivalent fluorine atoms, with appropriate T_1 and T_2 relaxation times, be scalable and easy to formulate, and be chemically inert and non-cytotoxic.[7]

Over the past three decades, many fluorinated materials have been prepared and studied as molecular imaging and therapeutic tracers. Since the late 90s, researchers started considering perfluorocarbons (PFCs) (i.e., organic compounds in which all hydrogen atoms are replaced with fluorine) for ^{19}F-MRI applications. Perfluorooctyl bromide (PFOB), perfluorononane (PFN), perfluorotributylamine (PFTBA), perfluoropropane (PFP), and perfluorodecalin (PFD) were first proposed as ^{19}F-MRI tracers. However, due to the high amount of nonequivalent fluorine atoms, they give multiple ^{19}F-MRI signals with different chemical shifts resulting in reduced local ^{19}F concentrations and chemical shift imaging

https://doi.org/10.1021/accountsmr.2c00203
Acc. Mater. Res. XXXX, XXX, XXX−XXX

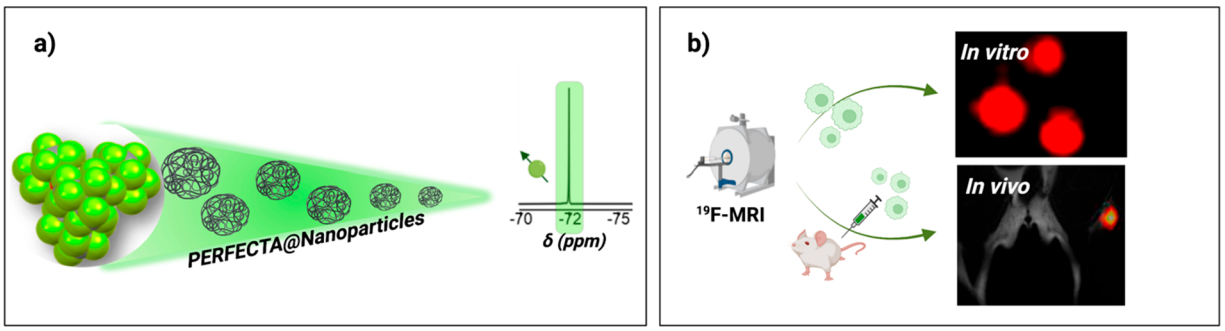

Figure 2. Crystal structure of PERFECTA molecule with a representation of a nanoformulation to disperse it in an aqueous solution showing a characteristic single intense ^{19}F-NMR signal (a) and enhanced sensitivity in both *in vitro* and *in vivo* ^{19}F-MRI (b). Reproduced with permission from ref 12. Copyright 2014 American Chemical Society.

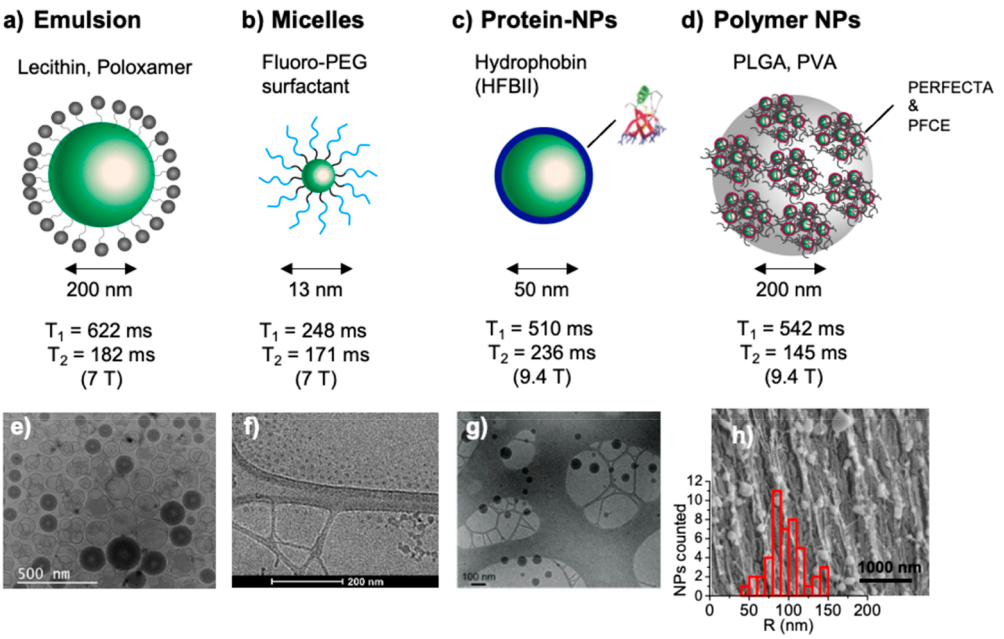

Figure 3. Overview of nanoformulations of PERFECTA for *in vivo* use with their characteristic sizes and relaxation times. (a) PERFECTA loaded NPs can be formulated with lipid-based (e.g., lecithin) and polymeric (poloxamer) systems. (b) Smaller micelles were obtained using a nonionic, PEG-based, fluorinated surfactant. (c) PERFECTA NPs stabilized with the amphiphilic protein Hydrophobin (HFB-II). Such NPs are expected to have reduced immunogenicity compared with PEG-based surfactants. (d) NPs with fractal structures were obtained using PLGA with poly(vinyl alcohol) (PVA) as surfactant. Here, PERFECTA was coloaded into NPs with PFCE for tracking their degradation. Cryogenic transmission electron microscopy (cryo-TEM) images of (e) @PERFECTA lecithin-stabilized NPs (scale bar 500 nm), (f) @PERFECTA PFTD-PEG micelles (scale bar 200 nm). Reproduced with permission from ref 22. Copyright 2021 The Royal Society of Chemistry. (g) @PERFECTA HFBII-FNPs (scale bar 100 nm). Reproduced with permission from ref 21. Copyright 2022 The Authors. *Advanced Materials Interfaces* published by Wiley-VCH GmbH. (h) @PERFECTA_PFCE fractal NPs (scale bar 1000 nm). Reproduced with permission from ref 23. Copyright 2020 The Authors. Published by Elsevier Inc.

artifacts.[3,7] For this reason, research moved toward the development of PFCs with a chemical design affording many-fold magnetically equivalent ^{19}F atoms, such as perfluoro-15-crown-5-ether (PFCE) used by Ahrens et al. in 2005 for tracking immunotherapeutic cells.[8] Linear perfluoropolyether (PFPE) mixtures with many "pseudo-equivalent" ^{19}F atoms were also proposed for ^{19}F-MRI.[9]

Today, the standards used for preclinical and clinical studies are PFOB, PFCE, and linear perfluoropolyether (PFPE) mixtures.[7] However, despite their widespread use in ^{19}F-MRI, they still suffer from several drawbacks. Given their strong amphiphobic behavior, in fact, PFCs require formulation processes to become suitable for administration as water solutions. Moreover, the strong C−F bonds in PFCs make them extremely stable. Thus, they tend to bioaccumulate and are raising sustainability concerns. Finally, PFCs are generally difficult to functionalize due to the lack of modifiable groups.[3,10]

In the search of novel ^{19}F-MRI tracers with improved physiochemical and biological properties, branched systems gained a lot of attention due to the possibility of bearing an elevated number of equivalent fluorine atoms, resulting in an improved ^{19}F-MRI sensitivity, as well as the reduced bioaccumulation concerns. In 2007, Yu and Jiang first identified and proposed perfluoro-*tert*-butanol (PFTB) as an ideal building block for ^{19}F-MRI tracers, thanks to its high content of equivalent ^{19}F atoms, together with easy availability and functionalization.[10,11] Later, in 2014, our group developed a biocompatible PFTB-based superfluorinated tracer, called PERFECTA, with 36 equiv fluorine atoms, which is nowadays

https://doi.org/10.1021/accountsmr.2c00203
Acc. Mater. Res. XXXX, XXX, XXX−XXX

considered one of the most effective ^{19}F-MRI ones. PERFECTA can easily be dispersed in physiological media through formulation with biocompatible additives, and the presence of ethereal bonds may hasten for enhanced biodegradability.[12] Moreover, PERFECTA's scaffold can be modified for producing partially fluorinated macromolecules with different topologies and features[13,14] (such as biodegradable polyesters and dendrimers), increasing system functionality[15] (such as nanoparticles and surfaces functionalization), and producing novel derivatives with improved features such as solubility and degradation (Figure 1).

In this Account, we will discuss the main challenges that fluorinated tracers need to overcome for their translation to clinic with a look at possible future perspectives in their customized design, aiming at the development of multifunctional materials for different still unexplored fields (i.e., multiscale, multicolor, and multimodal imaging). We envision that our strategy based on PERFECTA can be used for producing libraries of fluorinated molecules and colloidal materials acting as efficient ^{19}F-MRI and multimodal imaging tracers. We wish this Account to be of inspiration for the development of innovative and more effective ^{19}F-MRI tracers, pushing forward their clinical translation.

2. SUPERFLUORINATED TRACER (PERFECTA)

2.1. Synthesis, Formulation, and ^{19}F-MRI Application

PERFECTA's branched structure affords a high payload of chemically equivalent ^{19}F atoms (36/molecule) (Figure 2a), which give a single, intense, and well-resolved ^{19}F-NMR signal for enhanced sensitivity without chemical shift artifacts (Figure 2a,b).[3,12]

Moreover, it is a crystalline solid compound obtained by an easy and scalable synthesis procedure. Additionally, with its four ether bonds, it may allow for molecular degradation in the biological environment. In fact, multiple works demonstrated that ether bonds can be metabolized by oxidative degradation[16] in *tert*-butyl ether compounds.[17] Therefore, we envision that PERFECTA can potentially promote fast clearance, overcoming bioaccumulation issues[18] typical of many conventional and commercial PFCs.[19] However, further studies are currently in progress to confirm this hypothesis.

Due to its high fluorine content, despite not being perfluorinated, PERFECTA's fluorine atoms fully shield the pentaerythritol core structure, making it highly hydrophobic.[12] Therefore, it is necessary to formulate it for biomedical use, ensuring stability in the physiological milieu. Being solid at room temperature, established liquid PFC formulation procedures cannot be directly applied, thus requiring the development of different approaches. To date, we developed several types of colloidal formulations containing PERFECTA, which display optimal relaxation times, T_1 and T_2 and confirm its excellent suitability as ^{19}F-MR tracer (Figure 3a−h).[12,20,21]

The first explored route for dispersing PERFECTA in an aqueous environment was through a phospholipid-stabilized emulsion with lecithin and safflower oil.[12] These emulsions showed promising colloidal stability over 5−7 weeks. Nonionic surfactants were also used to form PERFECTA dispersions, as we have shown with Pluronic F68 (polyethylene glycol-*b*-polypropylene glycol-*b*-polyethylene glycol (PEG−PPG-PEG).[20] Both formulations yielded nanoparticles (NPs) of about 200 nm with monomodal distribution (Figure 3a,e). This size regime is typically used for *ex vivo* labeling of immune cells and for *in vivo* monitoring of inflammation by tracking mononuclear cell phagocytic activity.[6,20] However, for other applications such as *in vivo* guided therapy, in which NPs are administrated *i.v.* and need to localize in specific tissues, smaller sizes are necessary to reduce undesired clearance from the bloodstream. With this perspective, Jamgotchian et al. obtained PERFECTA loaded micelles of about 25 nm using a nonionic PEG-based surfactant bearing perfluorotridecanoate as the fluorophilic moiety to maximize the interaction with PERFECTA fluorinated chains (Figure 3b,f).[22] PEG-based surfactants typically display a stealth effect to ensure stability in the physiological milieu and reduce formation of protein corona, which is necessary to minimize undesired blood clearance.[24] However, it has been shown that PEG can lead to antibody formation, thus accelerating blood clearance,[25,26] promoting researchers to explore PEG alternatives.[24,27,28] Therefore, we explored a class of amphiphilic proteins, hydrophobins, as possible nonimmunogenic stabilizers for obtaining PERFECTA formulations with reduced sizes and stealth properties (Figure 3c,g).[21] Hydrophobin-II (HFBII) displays a highly hydrophobic patch enabling, for example, the formation of HFBII films on hydrophobic and fluorinated[29] switching surface.[30−32] This rationale was applied to disperse PERFECTA in HFBII aqueous solutions resulting in the formation of 50 nm PERFECTA solid NPs coated by a protein shell. HFBII enhances the stability of PERFECTA NPs in physiological media, reducing the adsorption of blood coagulation and immune response proteins in human plasma, which typically lead to unwanted blood clearance of injected NPs.

If reticuloendothelial system (RES) sequestration of PERFECTA loaded NPs from the bloodstream has to be avoided or at least delayed, fast clearance from accumulation organs should be guaranteed. In fact, bioaccumulation and long retention times are one of the concerns for the use of fluorinated tracers, as such a long accumulation prohibits repeated injections of the tracer making it indistinguishable from the first injection. In this regard, it was shown for another PFC, perfluoro-15-crown-5 ether (PFCE), that encapsulation in poly-lactic-*co*-glycolic acid (PLGA) NPs strongly accelerated PFCE organ clearance.[33−35] A structural characterization of such NPs showed a fractal structure, in which PFCE is dispersed in the polymeric matrix forming several small spheres, leading to a faster elimination from the organs through formation of smaller PFCE droplets upon degradation.[33−35] A faster clearance is beneficial for ^{19}F-MRI when repeated imaging sessions are needed, and required for clinical approval. With respect to this, we have succeeded to develop similar fractal PLGA NPs coloading PERFECTA with PFCE (Figure 3d,h).[23] Upon hydrolysis of these NPs, no segregation of the fluorous phase was observed, suggesting that PFCE-PERFECTA NPs break in smaller fractal domains, which should accelerate organ clearance. Interestingly, MR properties of the two tracers changed upon hydrolysis, suggesting that the degradation of these coloaded NPs can be tracked *in vivo* by MRI.[23] Thus, this system can be used in the future as an alternative approach to optical tracers[36] to detect degradation of drug delivery systems.

According to these results, the PERFECTA half-life could be further improved by exploiting the ultrastructure of polymeric formulations. Importantly, these polymeric NPs show excellent colloidal stability, high loading yields, and effective MRI properties as a reduced T_1 compared to those obtained with

https://doi.org/10.1021/accountsmr.2c00203
Acc. Mater. Res. XXXX, XXX, XXX−XXX

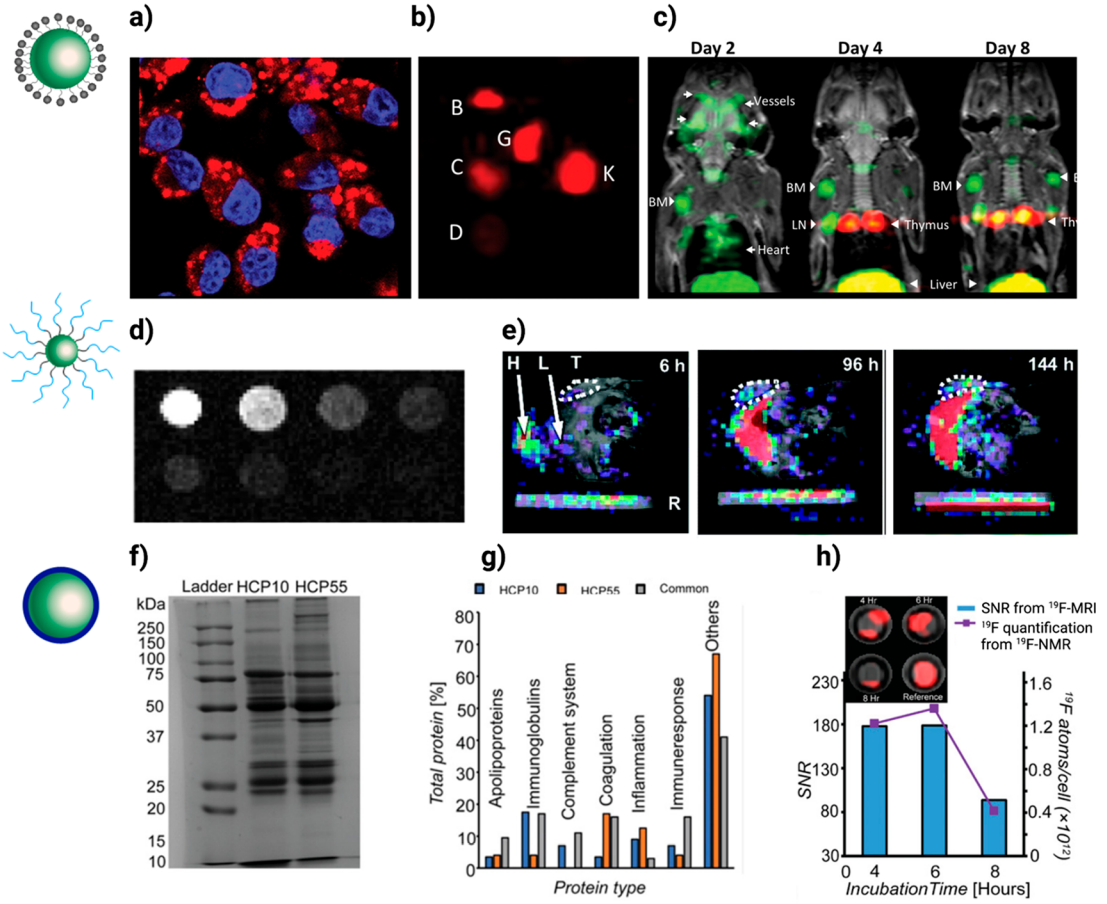

Figure 4. *In vitro* studies performed on microglial cells using Pluronic F68-stabilized PERFECTA-NPs. Both (a) confocal microscopy analysis and (b) ^{19}F-MRI (B and J, 8000 cells; C, H, and G, 16000 cells; F and K, 32000 cells) on labeled cells highlighted optimal ^{19}F labeling. (c) *In vivo* multicolor ^{19}F-MR acquisitions in control and mononuclear cell depleted mice at different days after interruption of the depletion diet and administration of either PFCE (green) or PERFECTA (red). Reproduced with permission from ref 20. Copyright 2019 RSNA. (d) Optimization of the imaging sequence used to efficiently image PERFECTA@PFTD-PEG micelles by ^{19}F-MRI. (e) Description of the *in vivo* imaging study performed in tumor-bearing mice after *i.v.* injection of PERFECTA loaded micelles; combined ^{1}H and ^{19}F-MRI images of diseased mice at specific timing from micelles administration (T = tumor; L = liver; H = heart; R = reference tube). Reproduced with permission from ref 22. Copyright 2021 The Royal Society of Chemistry. Analysis of the Protein Corona performed on HFBII-PERFECTA NPs. (f) SDS-PAGE of HC isolated after incubation of HFBII-NPs with10%, 55% human plasma (v/v). (g) Histograms comparing specific and common proteins identified in HCP10 and HCP55. Proteins were divided into seven categories, based on biological processes they are involved in. (h) ^{19}F cellular uptake quantified using both ^{19}F-NMR and ^{19}F-MRI (SNR) experiments for microglial cells labeled with HFBII-NPs for different incubation times. Reproduced with permission from ref 21. Copyright 2022 The Authors. *Advanced Materials Interfaces* published by Wiley-VCH GmbH.

earlier PERFECTA formulations, resulting in efficient imaging tracers.[12,20,21]

Tailoring composition, size, and surface modification allowed for the development of diverse PERFECTA NPs suitable to specific biomedical needs. For example, PERFECTA emulsions were successfully applied for imaging dendritic cells (Figure 4a,b) and studying inflammation progression *in vivo* by ^{19}F-MRI (Figure 4c). PERFECTA loaded micelles showed great ^{19}F-MR sensitivity (Figure 4d) and were specifically accumulated in the tumor by passive targeting after their intravenously injection (Figure 4e); accumulation in other organs, particularly in the liver, was also observed. Despite the still outstanding *in vivo* biodistribution study, present results in the biological milieu suggest that HFBII-stabilized PERFECTA NPs could be used as ^{19}F-MRI tracking tracers *in vivo* (Figure 4f–h).

2.2. Dual-Modal Imaging

PERFECTA, as other ^{19}F-MR sensitive tracers, is often combined in the formulation with fluorescence imaging agents, enabling analysis at the cellular level. Fluorescent labeling allows the determination of significant information at different detection scales with a high specificity. For example, by encapsulating PERFECTA with hydrophobic fluorescent probes, it is possible to characterize PERFECTA loaded cellular subsets that are mainly active and involved during the mononuclear cell regeneration after microglia depletion.[20]

More recently, we have proposed an alternative imaging approach for PERFECTA detection, sensitive at cell/tissue levels, without using additional fluorescent agents. In fact, the characteristic C−F Raman vibrational modes of PERFECTA fall in a cell silent region and can be used as a specific fingerprint of the molecule, enabling imaging by Raman microscopy.[37] PERFECTA can be used as multiscale imaging tracer, being active in both ^{19}F-MRI, on a whole-body scale, and Raman microscopy, on a tissue/cell scale (Figure 5a). While this specific Raman signature is shared by other standard ^{19}F tracers including PFCE and PFOB, PERFECTA shows the highest sensitivity both in ^{19}F-MRI and in Raman (Figure 5b).

https://doi.org/10.1021/accountsmr.2c00203
Acc. Mater. Res. XXXX, XXX, XXX−XXX

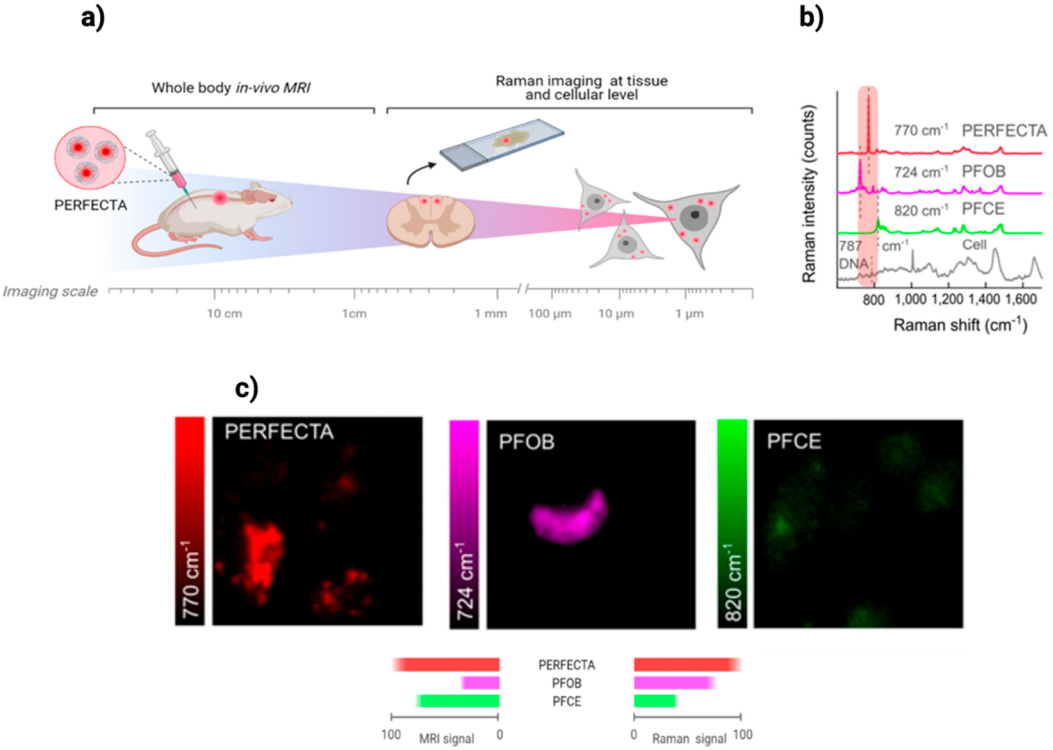

Figure 5. (a) Representation of PERFECTA-based bimodal imaging strategy. *In vivo* experiments showed this bimodal approach provides multiscale imaging from whole body to histological and subcellular size. (b) Raman spectra of PERFECTA-NPs compared to other fluorinated tracer nanoformulations (PFOB, PFCE) and typical Raman spectrum of mammal cells. (c) Raman imaging of *in vitro* labeled microglial cells with fluorinated nanoformulations (red, PERFECTA; purple, PFOB; green, PFCE) after selecting Raman signals of each tracer, organic matrix (1450 cm^{-1}), and DNA (787 cm^{-1}) (scale bar, 10 μm). Reproduced with permission from ref 37. Copyright 2021 The Authors. Published by American Chemical Society.

This enhanced efficiency is a consequence of the highest ^{19}F payload and symmetrical structure replicated over the four arms of the molecule, enabling its clear detection in the biological environment (Figure 5b,c). A unique multimodal tracer permits reliable correlations and avoids costly and laborious chemical strategies for the multicomponent nanoprobe development. Furthermore, the proposed strategy helps to overcome common drawbacks related to the coencapsulation of fluorescent dyes with the ^{19}F tracer such as dissociation from the ^{19}F NPs, and fluorescence quenching.

The bimodal ^{19}F-MRI/Raman PERFECTA-based approach can be extended to other fluorinated tracers and opens the way to support several needs of the ^{19}F-MRI tracers in biomedical research and clinical application, for instance monitoring progression of inflammation, tracking of therapeutic cells, promoting early diagnosis, personalized medicine, and precision surgery. Furthermore, considering that Raman spectroscopy provides additional label-free details due to the innate chemical fingerprint of the biological molecules, the molecular composition of the tissue where the fluorinated tracer is localized can also be assessed. This multimodality may not only determine the tracer biodistribution (^{19}F-MRI) but also provide unique information on the molecular composition of the biological environment, distinguishing healthy tissues from diseased regions (Raman microscopy). Importantly, all these advantageous applications could be easily extended to novel and more effective Raman labeling strategy, thanks to the versatile molecular design of PERFECTA and production of highly sensitive fluorinated derivatives.[15]

3. MULTIBRANCHED PARTIALLY FLUORINATED PERFECTA DERIVATIVES

As discussed in the above section, the hyperbranched structure of PERFECTA, characterized by short, fluorinated chains affording an elevated number of equivalent fluorine atoms, makes it one of the most promising ^{19}F-MRI tracers. At the same time, in the path for ^{19}F-MRI clinical translation, synergic efforts should be oriented toward the development of novel multifunctional fluorinated nanocomposites. Next generation fluorinated materials for bioimaging should indeed be versatile, with a broader solubility profile and able to integrate multiple groups in the same molecule, offering other functions besides ^{19}F-MRI (i.e., tissue/organ targeting, fast clearance, imaged drug delivery). By reducing the number of perfluoro-*tert*-butyl branches of PERFECTA, it is possible to synthesize synthons with different degrees of fluorination and terminal groups. This strategy paves the way for the functionalization of a variety of molecules and systems (from small peptides and bioactive agents to larger structures such as polymers, dendrimers, lipids, and NPs) with the development of ^{19}F-MRI sensitive macromolecules and nanosystems with improved functionalities. The strength of this approach relies on the possibility of tuning the characteristics of the final material, playing both on the degree of fluorination (by reducing the number of PERFECTA fluorinated branches) and on the different types of functional groups and substituents that can be linked to the resulting PERFECTA-based tags, allowing for the development of extremely versatile fluorinated compounds.

Currently, in the literature, the two main reported strategies in this context are based either on the development of tri-

https://doi.org/10.1021/accountsmr.2c00203
Acc. Mater. Res. XXXX, XXX, XXX−XXX

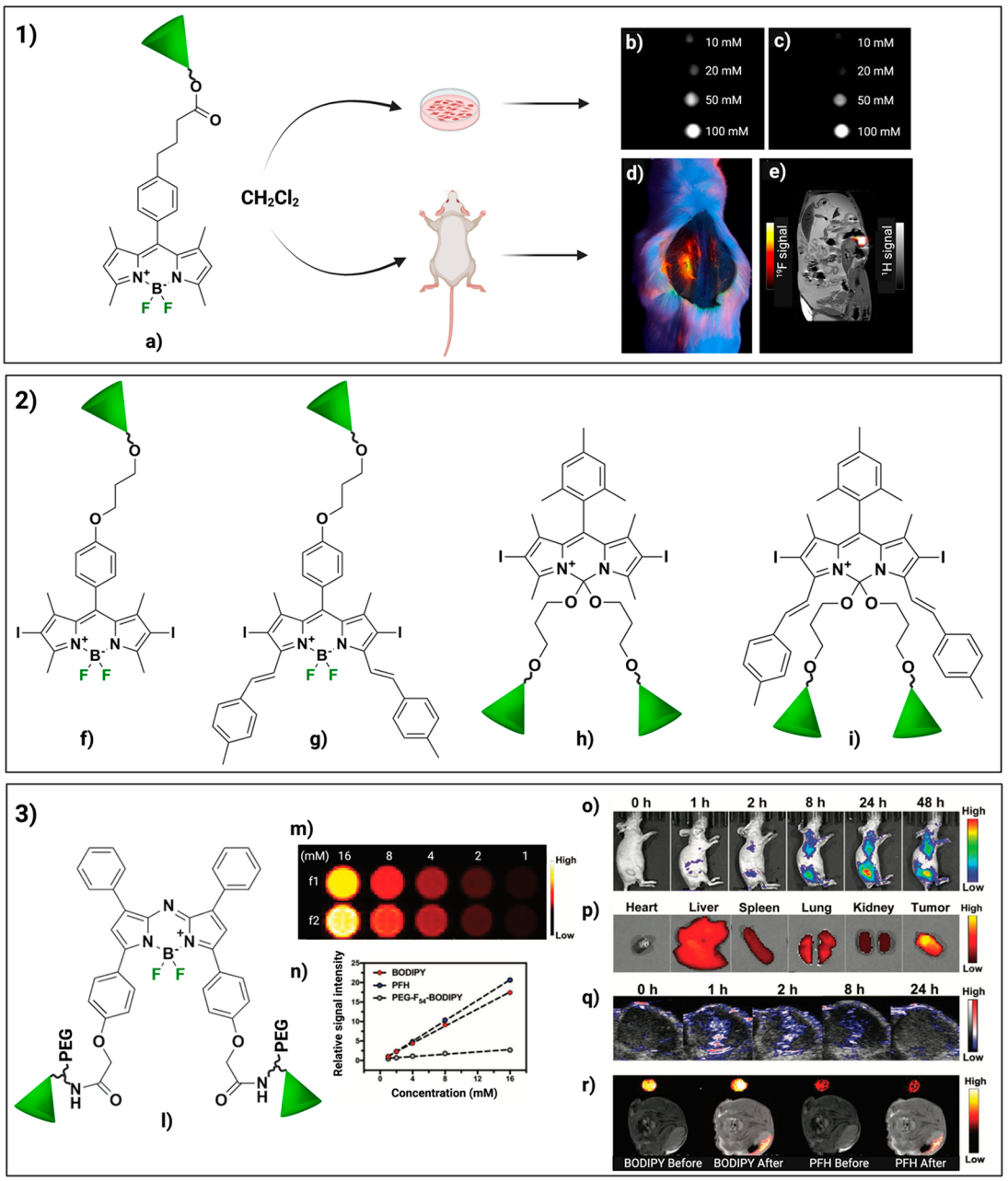

Figure 6. Examples of F27 functionalized BODIPY systems for bimodal (^{19}F-MRI/FLI) imaging application. (1) *In vitro* and *in vivo* tests of the compound in (a) at various concentrations. (b) ^{19}F-MRI FLASH and (c) RARE sequences of 10−100 mM concentrations. (d) Black light (λ_{exc} = 365 nm) excited fluorescence photograph of a mouse post-mortem, injected with 100 μL of 100 mM of the compound in (a) solution in CH_2Cl_2. (e) Overlay of ^{1}H (grayscale) and ^{19}F-MRI (color) images of the same mouse in (d). Reproduced with permission from ref 46. Copyright 2016 Wiley-VCH. (2) Examples of a series of BODIPY dyes functionalized with either one (f, g) or two (h, i) F27 derivatives. (3) Chemical and biological characterization of the compound in (l). (m) *In vitro* MR images and (n) corresponding MR signal intensity of the compound in (l) with PFH (f1, BODIPY; f2, PFH). (o) *In vivo* NIR FL images. (p) *Ex vivo* FL images. (q) Representative photoacoustic images. (r) ^{19}F-MRI of A375 tumor before and 30 min after the injection of the compound in (l) with PFH. Reproduced with permission from ref 45. Copyright 2019 Wiley-VCH.

PFTB functionalized pentaerythritol (F27) derivatives or on simpler systems with a single PFTB group (F9). The choice of the ideal strategy depends on the desired final properties of the system: balance between hydrophobicity and hindrance of the fluorinated part, the amount of equivalent fluorine atoms, and their mobility in the final system. These characteristics, as previously discussed, are all directly related to the sensitivity and effectiveness of a ^{19}F-MRI tracer and thus have to be carefully balanced in order to develop systems with potential clinical translation.

3.1. F27 Functionalized Molecules and Macromolecules

The strength of the F27 synthon mainly relies on the elevated number of equivalent fluorine atoms per molecule, on the highly branched structure of the fluorinated moiety, expected to be more environmentally friendly with respect to longer linear fluorinated chains, and on the plethora of potential chemical functionalization they can undergo.

https://doi.org/10.1021/accountsmr.2c00203
Acc. Mater. Res. XXXX, XXX, XXX−XXX

Since 2007, when Yu and Jiang first demonstrated the feasibility of synthesizing a broad range of F27 derivatives, for the development of multifunctional vehicles for ^{19}F-MRI guided targeted therapy,[11,38−41] the library of studied and developed F27-based materials has increased exponentially, as well as their use in different biological applications.

The functionalization of drugs and bioactive molecules with the F27-tag represents, for example, a promising approach for the development of traceable pharmaceutics.[10] Fluorination of bioactive agents is eventually reported to change their physiochemical properties and modulate their interaction with the biological environment. In particular, the simultaneous hydrophobic and lipophobic features of fluorinated chains enhance membrane penetration and endosomal escape, as well as tissue permeability, and result in an increased cellular uptake of fluorinated drugs, genes, proteins, and peptides.[42] This strategy was for example adopted by Shi et al., who reported the functionalization of 4-anilinoquinazoline with F27 for the development of ^{19}F-MRI traceable EGFR tyrosine kinase inhibitors.[43] Despite promising opportunities offered by such an approach, the clinical translation of ^{19}F-MRI traceable bioactive compounds is mainly hampered by the hard task of balancing their bioactivity with ^{19}F-MRI sensitivity. Indeed, a safe *in vivo* concentration of the bioactive agent is usually one order less than the necessary ^{19}F concentration for effective ^{19}F-MRI.[10] Although the use of the F27-tag, thanks to the high number of equivalent fluorine atoms, might be an effective strategy for reducing sensitivity issues, more efforts are needed for developing clinically effective ^{19}F-MRI traceable bioactive tracers. The sensitivity problem can also be supported by the use of high-field MRI scanner and cryogenic radiofrequency probes.[44]

Labeling with F27 units is a valuable route also to develop systems for bimodal and multimodal imaging applications. The combination of the F27 synthon with a fluorescent dye is the conventional strategy to tackle this purpose. Different F27 derivatives functionalized with fluorescent molecules (such as boron dipyrromethene dyes, BODIPY) have indeed been proposed as fluorescence imaging (FLI)/^{19}F-MRI bimodal tracers.[10] These systems are particularly promising as they allow for simultaneous *in vivo* tracking (^{19}F-MRI) and *ex vivo* intracellular localization. Additionally, the functionalization of the BODIPY core permits tuning the emission spectra to the near-infrared (NIR) region, allowing also for efficient photoacoustic imaging, and thus gives the possibility to develop effective potential multimodal systems.[45] In 2016, Huynh et al., proposed an F27 alcohol derivative functionalized with a BODIPY suitable for combined FLI and ^{19}F-MRI imaging (Figure 6, panel 1). The reported system was able to produce a bright ^{19}F-MRI signal at low concentration values (in agreement with previously reported detection limits in the field), as well as a strong FLI signal in a mouse post-mortem.[46] On the same line, in 2019 we reported the synthesis and characterization of a series of BODIPY dyes functionalized with either one or two F27 tags, representing good candidates as potential dual-imaging tracers for FLI and ^{19}F-MRI applications (Figure 6, panel 2).[13]

It is important to consider that the functionalization of fluorescent dyes with F27 tags further reduces their already limited water solubility, so that they are required to be formulated with surfactants or emulsifiers for their biological use. One possible way to manage this issue is to design F27-BODIPY structures bearing covalently bound additional hydrophilic moieties, such as PEG chains (Figure 6, panel 3).[45] However, the resulting derivatives acquire amphiphilic properties and self-assembly that can lead to a decrease in the mobility of the fluorinated chains, which negatively affects the ^{19}F-MRI signal and consequently the potential bimodality of the system. In this regard, Zhang et al. recently showed that addition of perfluorohexane (PFH) to a solution of a PEG-F_{54} functionalized BODIPY amphiphile effectively enhanced its ^{19}F-MRI signal, with respect to the pristine formulation. PFH was indeed able to interact with the fluorinated chains of the tracer, enhancing their mobility and thus improving the T_2 relaxation time.[45]

F27-BODIPY bimodal systems clearly have a strong potential for biomedical applications, in particular for the fluorescence-guided surgery by coupling to NIR-emitting fluorophores. However, the previously mentioned issues regarding reduction in their relaxivity performance upon formulation processes raises the need of carefully evaluating this strategy. Indeed, considering the Raman-responsiveness recently demonstrated for PERFECTA,[37] which applies also to F27 tags, they are intrinsically bimodal imaging agents. It is thus possible to develop simpler bimodal systems, having the F27 synthon as a unique "active" moiety, avoiding eventual degradation or detachment of the fluorescent molecule from the fluorinated core with misleading information due to different biological localizations of the two imaging-active moieties.

In the attempt to combine a high degree of fluorination with improved water solubility or dispersibility, much effort has been dedicated to the development of bimodal fluorinated systems obtained by functionalizing hydrophilic polymers and dendrimers with fluorinated tags. By varying the type of polymer and dendrimer scaffolds, it has been possible to confer different properties to the system, in terms of biodegradability, biocompatibility, and level of hydrophilicity. The resulting systems are often amphiphilic. Thus, they spontaneously self-assemble in aqueous solutions, with enhanced attitude to interact with cell membranes and consequent higher cellular internalization.[47] Moreover, these amphiphilic supramolecular assemblies can encapsulate both hydrophobic and hydrophilic drugs, thus having the possibility to act as ^{19}F-MRI traceable drug or gene delivery vehicles. This strategy could represent a valuable alternative with respect to previously discussed direct functionalization of the bioactive molecules with F27 tags.

Among the different examples of F27 functionalized hydrophilic polymers and dendrimers reported in the literature, the work by Decato et al., notably showed that a single PEG chain functionalized with F27 moieties was able to form stable spherical micelles in aqueous media with favorable MRI properties. The ability of these assemblies to effectively emulsify 20% (v/v) of the highly fluorinated anesthetic sevoflurane make them potentially useful as theranostic agents.[48]

Besides linear-chain polymers, other valuable scaffolds for the development of high-performance ^{19}F-MRI tracers are offered by multibranched macromolecules and dendrimers thanks to their peculiar 3D structures and better control on synthesis and structure modification procedures. One of the first attempts in this sense was a water dispersible F27 branched derivative functionalized with four short polyethylene glycol (PEG) chains, termed ^{19}FIT, reported by Jiang et al. in 2009. Despite its good water solubility (CMC ∼ 7 mM in PBS), good biocompatibility, and rapid body

https://doi.org/10.1021/accountsmr.2c00203
Acc. Mater. Res. XXXX, XXX, XXX−XXX

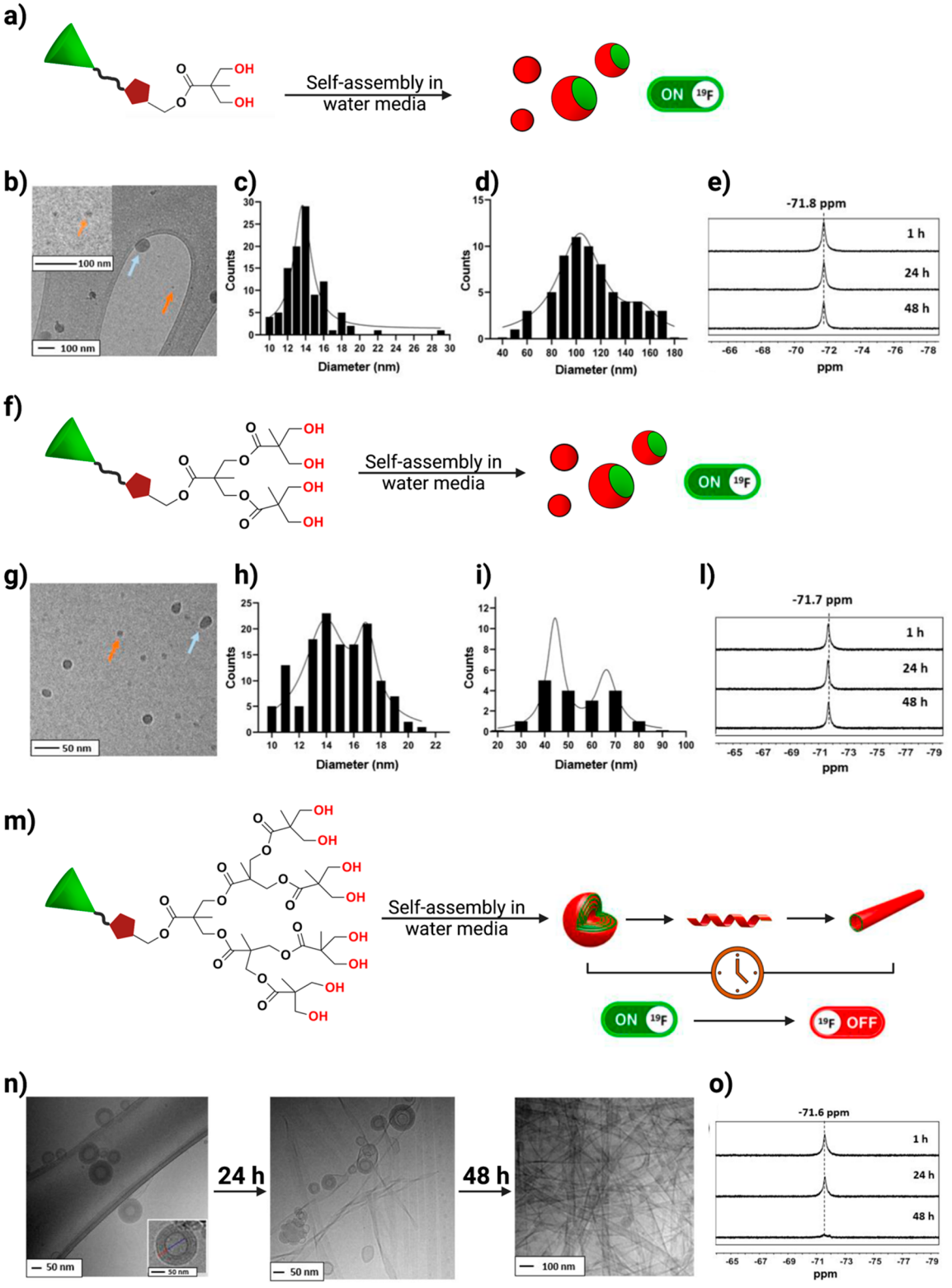

Figure 7. Biodegradable fluorinated Janus type dendrimers. (a) F27 functionalized dendrimer of generation I. (b) cryo-TEM images showing the presence of bigger NPs (light blue arrow) and smaller systems, i.e., micelles (orange arrow). (c) and (d) size distributions of smaller and larger NPs from cryo-TEM images. (e) ^{19}F-NMR spectra over time. (f) F27 functionalized dendrimer of generation II. (g) Cryo-TEM images showing the presence of large spherical NPs (light blue arrow) and small micelles. (h) and (i) size distribution of larger and smaller NPs from cryo-TEM images. (l) ^{19}F-NMR spectra over time. (m) F27 functionalized dendrimer of generation III. (n) Cryo-TEM images showing the presence of multilamellar dendrimersomes fusing together after 24 h to form a sheetlike structure that after 48 h converted to tubules. (o) ^{19}F-NMR spectra over time, showing a quenching of the signal after 48 h. Reproduced with permission from ref 14. Copyright 2022 The Authors. Published by American Chemical Society.

https://doi.org/10.1021/accountsmr.2c00203
Acc. Mater. Res. XXXX, XXX, XXX−XXX

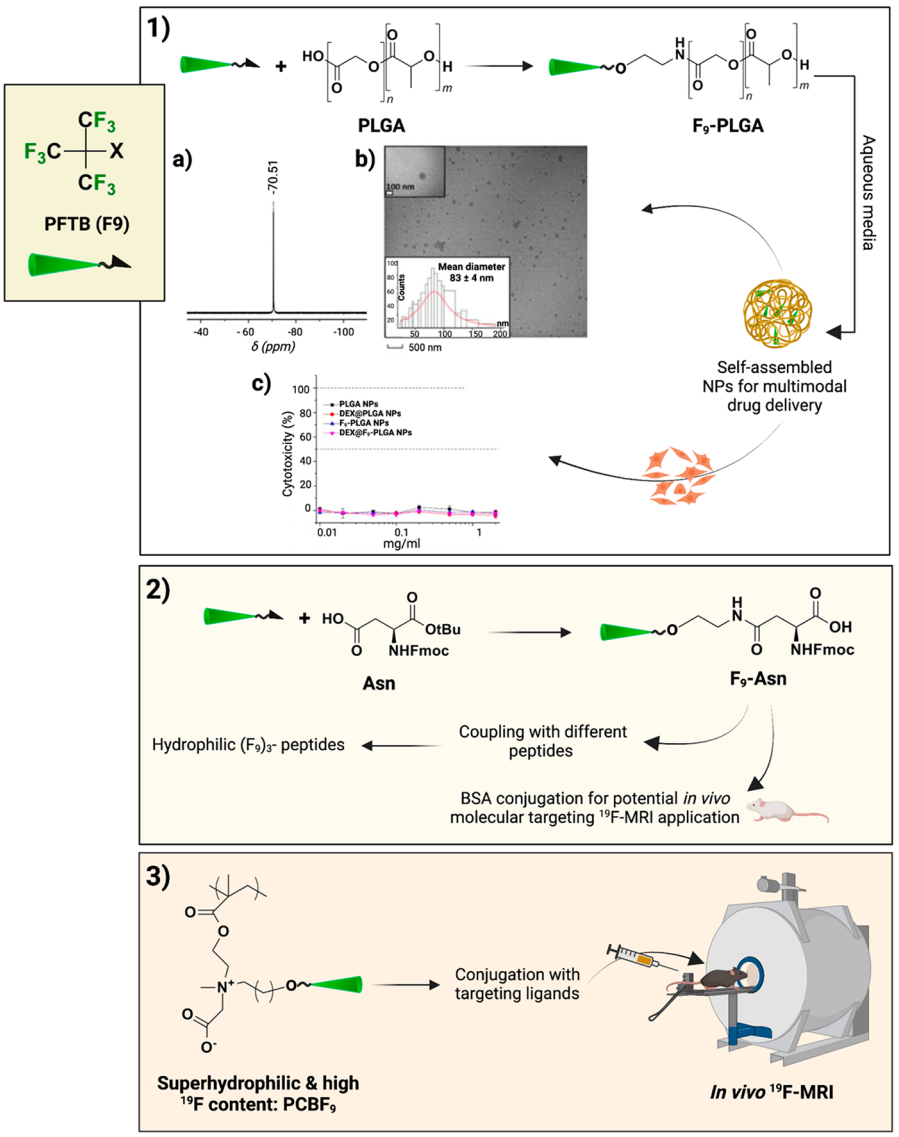

Figure 8. Examples of PFTB (F9) functionalized molecules. (1) ^{19}F-NMR spectra (a) and TEM images (b) of a dispersion of F_9-PLGA. LDH assay on HCIPodo cells (c) incubated with NPs (PLGA, F_9-PLGA, DEX@F9-PLGA) for 24 h. Reproduced with permission from ref 51. Copyright 2020 Wiley-VCH. (2) Schematic representation of Fmoc protected F_9-Asn and its possible functionalization with different peptides to obtain highly fluorinated peptides bearing different PFTB groups. (3) Schematic representation of a superhydrophilic ^{19}F-MRI CA, for target detection and computational quantification.

excretion, the ^{19}F-MRI performance of such derivatives was not optimal in terms of sensitivity.[39] Some years later, Taraban et al. synthesized a slightly different F27 functionalized amphiphilic dendrimer, whose terminal PEG chains underwent a concentration-dependent intramolecular conformational transition, instead of micellization. The concomitant ^{19}F chemical shift change suggests the possibility of developing stimuli-responsive tracers and might be useful for future ^{19}F-MRI traceable concentration-triggered drug release applications.[49]

Recently, we obtained a new family of fluorinated Janus-type dendrimers, with the F27 tag bound to bis-MPA (2,2-bismethylolpropionic acid) polyester dendrons of different generations, with tunable aggregation behavior and MRI response. Interestingly, it was possible to modulate their self-assembly in aqueous media by increasing the size, flexibility, and number of peripheral hydroxyl groups. If, on one hand, low generation dendrimers formed micelles with a high ^{19}F-NMR signal-to-noise ratio and signal stability over time, the highest generation derivatives underwent a morphological transition from multilamellar vesicles to tubules, with consequent reduction of fluorinated chains' mobility and switching-off of the NMR signal (Figure 7a–o).[14]

Analogous systems based on F27-tagged oligoglycerol dendrons were also successfully synthesized. When the linker between the fluorinated and hydrophilic sides was changed, self-assembly in water of these nonionic branched amphiphiles gave either multivesicular and multilamellar vesicles, or smaller unilamellar vesicles. In all cases, the resulting supramolecular architectures showed negligible cytotoxicity and good potential for drug delivery applications.[50]

3.2. F9 Functionalized Molecules

All the previously discussed examples underline the versatility of F27 derivatives in the development of ^{19}F-MRI tracers with improved functionalities. F27-based systems, indeed, maintain

https://doi.org/10.1021/accountsmr.2c00203
Acc. Mater. Res. XXXX, XXX, XXX−XXX

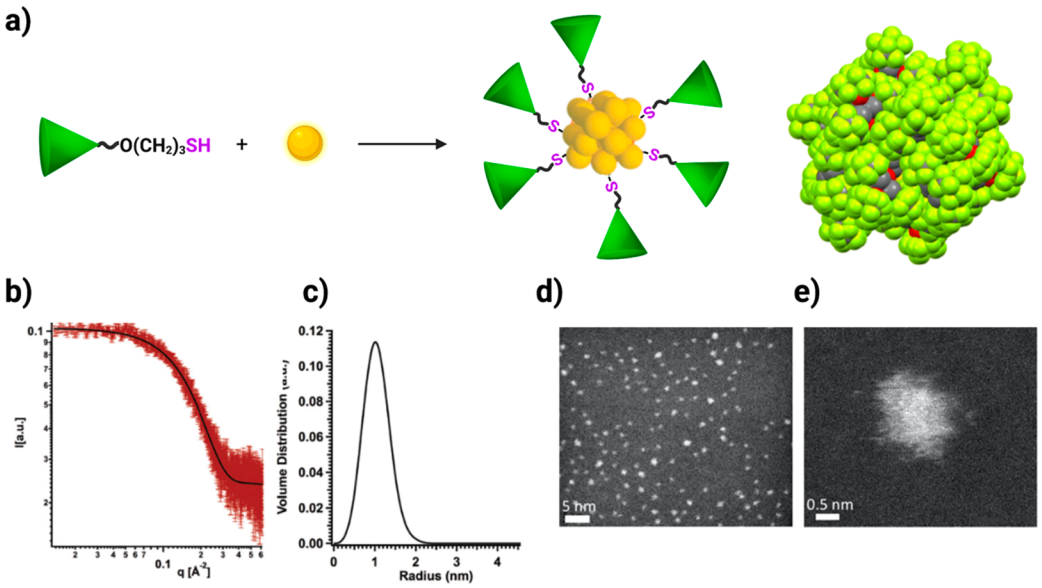

Figure 9. (a) Thiol terminated F27 derivative for the functionalization of ultrasmall gold NPs with the consequent formation of superfluorinated gold nanoclusters. Adapted with permission from ref 56. Copyright 2022 The Authors. (b) SAXS spectrum and (c) size distribution of radius size from SAXS obtained GIFT. Reproduced with permission from ref 15. Copyright 2017 The Royal Society of Chemistry. (d,e) STEM images of superfluorinated gold nanoclusters. Reproduced with permission from ref 56. Copyright 2022 The Authors.

an elevated number of equivalent fluorine atoms, suitable for effective ^{19}F-MRI application, and at the same time can be functionalized with different linkers and reactive groups that confer additional properties, such as multimodal responsivity, bioactivity, and amphiphilicity. However, it is also true that the presence of so many fluorine atoms can consistently lower their solubility and dispersibility in water and thus negatively affect their *in vivo* application.

For this reason, in parallel to F27 functionalized tracers, research efforts are being devoted also to the development of simpler derivatives bearing only one PFTB group (F9). This approach can be useful for increasing the water solubility of the resulting compounds, thanks to the reduction of the number of fluorinated branches, ensuring in any case an amount of equivalent fluorine atoms suitable for the needs of ^{19}F-MRI. Besides the solubility issue, a further limitation that was reported for some F27 derivatives is the quenching of their MRI signal once they are dispersed in solution, likely due to the reduced mobility of ^{19}F atoms in the final assemblies. On the other hand, similar substrates functionalized with smaller F9 moieties were not affected by this phenomenon, as we recently demonstrated for poly(lactic-*co*-glycolic acid) (Figure 8, panel 1).[51] Beyond an improved ^{19}F-NMR signal, the resulting self-assembled systems showed additional good encapsulation efficacy, in particular toward fluorinated drugs, thanks to the huge number of stabilizing F···F interactions occurring between the drug and fluorinated moiety of the PLGA.[51] This underlines the feasibility of some F9 functionalized molecules to work as effective ^{19}F-MRI sensitive drug delivery carriers, as discussed also for F27 derivatives. An interesting example of F9-labeling strategy for *in vivo* ^{19}F-MRI was lately achieved using fluorinated hydrophilic short peptide tracers (Figure 8, panel 2). Three F9 groups were introduced into asparagine analogues by amide bond linkages, and D-stereoisomers of charged amino acids were inserted in the peptide sequence in order to ensure high water solubility and stability against degradation. The additional presence of β-alanine residues endowed the peptide tracers with low cytotoxicity and high serum stability. The resulting unstructured peptides had all 27 ^{19}F atoms chemically equivalent, rendering them extremely promising candidates for *in vivo* imaging.[52] In the same year, Feng et al. reported a series of superhydrophilic fluorinated polymers, distinctly different from the more common superhydrophobic or amphiphilic ones, some of them functionalized with a PFTB group, showing promising results for ^{19}F-MRI application (Figure 8, panel 3).[53]

It, thus, seems that the choice of simpler and less fluorinated F9 derivatives can sometimes be a valuable option for developing effective ^{19}F-MRI tracers, as recently highlighted by Wu et al.[10]

Parallel to this, another reported approach, instead of playing with single PFTB units, focuses on single CF_3 units, covalently binding them to polymers and macromolecules obtaining promising results.[54,55]

According to the kind of application pursued, the most proper balance between the high degree of fluorination and structural mobility must be found to achieve optimal imaging performance in biological environments.

3.3. Functionalization of Inorganic NPs for ^{19}F-MRI

Most of the bioconjugate and bimodal F27/9-tagged systems discussed in the previous paragraph require additional formulation steps either to be dispersed in aqueous environments (e.g., F27-bearing drugs, biomolecules, or BODIPYs) or to spontaneously self-assemble into water-soluble MRI-active nanoaggregates (as in the case of F27/9 functionalized polymers or dendrimers).

Another strategy could be offered by the development of hybrid systems based on preformed NPs, such as inorganic NPs, whose surface is decorated with F27/9 tags. In principle, this approach could allow researches to develop theranostic platforms, combining the intrinsic features of the NP itself (such as photoreactivity, hyperthermia, imaging properties, etc.) with ^{19}F-MRI responsivity of the F27 synthon.

https://doi.org/10.1021/accountsmr.2c00203
Acc. Mater. Res. XXXX, XXX, XXX−XXX

In the synthesis of F-coated NPs, several aspects, including the NP dimensions, the packing parameter of fluorinated groups, and the length of the linker chain, have to be carefully designed, in order to avoid the limited mobility of ^{19}F atoms in the final system, loss of magnetic equivalence (multiple peaks), and consequently a reduced ^{19}F-MRI signal. If solid NPs can be functionalized on their surface with fluorinated groups, it will probably change their dispersibility in aqueous solutions. Among different kinds of NPs, gold NPs, thanks to their easy preparation and functionalization routes, have been the most used in this field. Moreover, gold NPs, depending on their shape and size, can afford optical and photothermal properties.[10]

In recent years, for instance, we decided to exploit the high affinity toward metals of a thiol terminated F27 derivative, which we already demonstrated in the case of planar surfaces,[18] for stabilizing gold NPs. Due to the highly branched and bulky structure of F27-SH, the synthesis led to the formation of ultrasmall highly fluorinated NPs (mean diameter <2 nm), termed gold nanoclusters, endowed with peculiar molecule-like optical properties, instead of the usual plasmon (Figure 9a–e).[15] In particular, their NIR photoluminescence and good ^{19}F-MRI properties might be promising for a bimodal imaging platform, after optimization of a suitable protocol for dispersing them in water. Moreover, spontaneous crystallization of such particles allowed us to confirm their atomically precise structure, which proved to be composed of a Au_{25} cluster core coated by a fully fluorinated shell of 18 F27-thiol molecules.[56] However, using these highly fluorinated NCs as bimodal imaging platforms requires their further formulation for allowing dispersibility in aqueous solutions. In this sense, recently Carril et al. have shown the functionalization of small core-sized Au NPs with F9 group linked to PEGylated ligands affording high F payload and good relaxivity properties.[57]

4. CONCLUSIONS AND OUTLOOK

In the current quest for new approaches for early diagnosis and the gradual tendency toward a more personalized medicine, medical imaging plays a central role. Among available imaging techniques, ^{19}F-MRI has been attracting increasing interest over the two last decades and much effort has been expended for its clinical translation. The strength of ^{19}F-MRI resides in the lack of endogenous fluorine in the human body, which allows for the quantitative detection of labeled cells/NPs as *hot-spot* images. However, its application into clinic is often hampered by sensitivity issues, which have stimulated consistent efforts for the customized development of increasingly effective ^{19}F-MRI tracers.

In this Account, while critically analyzing the main issues that are still preventing ^{19}F-MRI clinical translation, we have proposed our strategy based on PFTB-based tracers as a possible way for producing innovative ^{19}F-MRI traceable molecules and nanomaterials pushing forward the research in this field. The strong point of using these derivatives mainly relies on the elevated number of equivalent fluorine atoms, resulting in a single, intense, and well-resolved ^{19}F-NMR signal, on its easy and scalable synthesis procedure, and on its branched structure with four ether bonds (potentially metabolizable by oxidative degradation *in vivo*) that may allow for a faster clearance with respect to PFCs, overcoming bioaccumulation and sustainability concerns.

The PFTB-based approach permits the production of either fully fluorinated molecules (i.e., PERFECTA) or scaffolds (i.e., F9 and F27 tags) providing a vast range of macromolecules and nanomaterials with improved versatility and functionalities. In the former case, due to the high degree of fluorination of PERFECTA, formulation processes are required for biological use and protocols using different additives have been developed, all yielding NPs characterized by optimal relaxivity properties. On the other side, the ultrastructure of the final NP seems to have an important effect on the clearance of the fluorinated tracer; thus, more efforts should be dedicated to perform biodistribution studies of PERFECTA formulations with NPs characterized by different internal structures. The obtained results might get insights on the relation between the NP internal structure and clearance process of the fluorinated tracer, helping to optimize the formulation for avoiding bioaccumulation issues.

On the other side, by playing with the degree of fluorination, picking between the tri-PFTB functionalized pentaerythritol (F27) tag and a simpler PFTB group (F9), and picking the substituents linked to the chosen fluorinated synthon, it is possible functionalizing hydrophilic polymers and dendrimers, biomolecules, and drugs. The obtained derivatives often acquire amphiphilic properties forming assemblies of different shapes and sizes with an increased attitude toward lipid membranes and an enhanced cellular internalization. However, self-assembling F27 functionalized systems, combining the high degree of fluorination with good water dispersibility, can show a reduced ^{19}F-MRI response due to a lower mobility of the fluorinated chains in the aggregate state. This issue can be mitigated by either developing stimuli-responsive self-assembling systems, which for example disassemble upon cellular internalization with consequent activation of the signal, or reducing the ^{19}F payload using derivatives with a lower fluorination degree, such as F9 tags.

Another exciting progress in this field, recently reported by our group, is the innate Raman fingerprint of fluorinated tracers, which allows for their use as bimodal multiscale ^{19}F-MRI/Raman tracers. In this context, PERFECTA- and PFTB-based derivatives showed a sharper and more intense Raman signal than other PFCs enabling their *ex vivo* detection in tissues. Thus, in parallel to potential clinical applications, this intrinsic bimodality can strongly support several needs in preclinical studies for their further development without using additional fluorescent tags/probes (i.e., monitoring the progression of inflammation, tracking of therapeutic cells, promoting early diagnosis, personalized medicine, and precision surgery).

Overall, we strongly believe that PFTB-based derivatives are promising tracers for medical imaging and their further development in increasingly effective and sustainable materials can strongly support the translation of ^{19}F-MRI into clinic.

AUTHOR INFORMATION

Corresponding Authors

Pierangelo Metrangolo − *SupraBioNanoLab, Department of Chemistry, Materials and Chemical Engineering "Giulio Natta", Politecnico di Milano, Milan 20131, Italy;* orcid.org/0000-0002-7945-099X; Email: pierangelo.metrangolo@polimi.it

Francesca Baldelli Bombelli − *SupraBioNanoLab, Department of Chemistry, Materials and Chemical Engineering "Giulio Natta", Politecnico di Milano, Milan*

https://doi.org/10.1021/accountsmr.2c00203
Acc. Mater. Res. XXXX, XXX, XXX−XXX

20131, Italy; orcid.org/0000-0001-8138-9246;
Email: Francesca.baldelli@polimi.it

Authors

Beatrice Lucia Bona − *SupraBioNanoLab, Department of Chemistry, Materials and Chemical Engineering "Giulio Natta", Politecnico di Milano, Milan 20131, Italy;* orcid.org/0000-0002-7363-8756

Olga Koshkina − *Sustainable Polymer Chemistry Group, Department of Molecules and Materials, Mesa+ Institute for Nanotechnology, University of Twente, Twente 7522 NB, The Netherlands;* orcid.org/0000-0002-1202-6465

Cristina Chirizzi − *SupraBioNanoLab, Department of Chemistry, Materials and Chemical Engineering "Giulio Natta", Politecnico di Milano, Milan 20131, Italy;* orcid.org/0000-0002-8636-466X

Valentina Dichiarante − *SupraBioNanoLab, Department of Chemistry, Materials and Chemical Engineering "Giulio Natta", Politecnico di Milano, Milan 20131, Italy;* orcid.org/0000-0002-2977-5833

Complete contact information is available at: https://pubs.acs.org/10.1021/accountsmr.2c00203

Notes

The authors declare no competing financial interest.

Biographies

Beatrice Lucia Bona is currently a Ph.D. candidate in Industrial Chemistry and Chemical Engineering at Politecnico di Milano (Milan, Italy). She obtained a master's degree in Biomedical Engineering (Cells, Tissues, and Biotechnology specialization) from Politecnico in 2020 with a thesis related to the development of fluorinated dendrimers as gene delivery vehicles for the treatment of Amyotrophic Lateral Sclerosis. Her current research focuses on the development of fluorinated nanosystems for controlled drug delivery to the diseased heart.

Olga Koshkina (University of Twente) leads the research on polymer colloids for imaging and therapeutic use within the Sustainable Polymer Chemistry Chair supported by Alexander von Humboldt Foundation. She obtained her Ph.D. from the Technical University Berlin, with Fraunhofer IMM and Federal Institute for Materials Research. She then moved for postdoc to Radboud University Medical Center in Nijmegen (NL), and subsequently to the Max Planck Institute for Polymer Research before starting her group at the UT.

Cristina Chirizzi received her M.S. degree in Molecular Biotechnology in 2013 from the University of Turin. Since 2014 she has worked at IRCCS Ospedale San Raffaele, first as Ph.D. student and then as a postdoc fellow, focusing on the development of ^{19}F-MRI methods to image immune cells activity in preclinical models of multiple sclerosis. In March 2020 she joined the Laboratory of Supramolecular and Bio-Nanomaterials (SBN Lab) at Politecnico di Milano as Post-Doc fellow. Her research interests are focused on the development of nanoscale materials as ^{19}F tracers and/or drug carriers, diagnostic/theranostic systems.

Valentina Dichiarante is Associate Professor of Chemistry at Politecnico di Milano (Milan, Italy). She obtained a Ph.D. degree in Chemistry from the University of Pavia (Italy) in 2008. Prior to her appointment as Assistant Professor at Politecnico (2015-2021), she has been a postdoctoral researcher at University of Pavia (2008−2009), Commissariat à l'Energie Atomique et aux Energies Alternatives CEA-Saclay (France, 2010-2011), and Politecnico di Milano (2012−2015). Her current research interests focus on the development of highly fluorinated nanostructured and supramolecular functional materials.

Pierangelo Metrangolo is Professor of Fundamentals of Chemistry for Technologies at the Department of Chemistry, Materials, and Chemical Engineering "Giulio Natta" of Politecnico di Milano, Italy. Metrangolo holds a MSc degree in pharmaceutical chemistry and technologies from the University of Milan and a Ph.D. degree in industrial chemistry and chemical engineering from Politecnico di Milano, where he was appointed as a faculty member in 2002. His recent awards include the 2021 Giorgio Modena medal of the Italian Chemical Society and the 2019 Fluorous Technologies Award. His current research interests are supramolecular chemistry, crystal engineering, fluorine chemistry, peptides, and nanomedicine

Francesca Baldelli Bombelli is associate professor in Chemistry at Politecnico di Milano. She obtained the Ph.D. in Chemical Sciences in 2004 at University of Florence. After a Post-Doctoral training at University of Florence and University College Dublin she became Lecturer in Colloid Science and Nanotechnology at University of East Anglia (2011-2014) and Team Leader at the European Center of Nanomedicine in Milan. Her research interests include the development of fluorinated nanomaterials for drug delivery and imaging applications.

■ ACKNOWLEDGMENTS

The authors are thankful to the NEWMED project, ID: 1175999 (funded by Regione Lombardia POR FESR 2014 2020). F.B.B. and P.M. are also thankful to the project NiFTy funded by MIUR (PRIN2017, no. 2017MYBTXC). C.C., V.D., and F.B.B. are also thankful to the P2RY12 project, ID: GR-2016-02361325 (funded by the Italian Ministry of Health). O.K. acknowledges the Alexander von Humboldt Foundation. The figures were made using BioRender.com.

■ REFERENCES

(1) Davies, J.; Siebenhandl-Wolff, P.; Tranquart, F.; Jones, P.; Evans, P. Gadolinium: Pharmacokinetics and Toxicity in Humans and Laboratory Animals Following Contrast Agent Administration. *Arch. Toxicol.* **2022**, *96* (2), 403−429.

(2) Wei, Y.; Yang, C.; Jiang, H.; Li, Q.; Che, F.; Wan, S.; Yao, S.; Gao, F.; Zhang, T.; Wang, J.; Song, B. Multi-Nuclear Magnetic Resonance Spectroscopy: State of the Art and Future Directions. *Insights Imaging* **2022**, *13* (1), 135.

(3) Tirotta, I.; Dichiarante, V.; Pigliacelli, C.; Cavallo, G.; Terraneo, G.; Bombelli, F. B.; Metrangolo, P.; Resnati, G. 19 F Magnetic Resonance Imaging (MRI): From Design of Materials to Clinical Applications. *Chem. Rev.* **2015**, *115* (2), 1106−1129.

(4) Ruiz-Cabello, J.; Barnett, B. P.; Bottomley, P. A.; Bulte, J. W. M. Fluorine (19F) MRS and MRI in Biomedicine. *NMR Biomed.* **2011**, *24* (2), 114−129.

(5) Bulte, J. W. M. In Vivo MRI Cell Tracking: Clinical Studies. *Am. J. Roentgenol.* **2009**, *193* (2), 314−325.

(6) Ahrens, E. T.; Bulte, J. W. M. Tracking Immune Cells in Vivo Using Magnetic Resonance Imaging. *Nat. Rev. Immunol.* **2013**, *13* (10), 755−763.

(7) Zhang, C.; Yan, K.; Fu, C.; Peng, H.; Hawker, C. J.; Whittaker, A. K. Biological Utility of Fluorinated Compounds: From Materials Design to Molecular Imaging, Therapeutics and Environmental Remediation. *Chem. Rev.* **2022**, *122* (1), 167−208.

(8) Ahrens, E. T.; Flores, R.; Xu, H.; Morel, P. A. In Vivo Imaging Platform for Tracking Immunotherapeutic Cells. *Nat. Biotechnol.* **2005**, *23* (8), 983−987.

(9) Boehm-Sturm, P.; Mengler, L.; Wecker, S.; Hoehn, M.; Kallur, T. In Vivo Tracking of Human Neural Stem Cells with 19F Magnetic Resonance Imaging. *PLoS One* **2011**, *6* (12), e29040.
(10) Wu, T.; Li, A.; Chen, K.; Peng, X.; Zhang, J.; Jiang, M.; Chen, S.; Zheng, X.; Zhou, X.; Jiang, Z.-X. Perfluoro- Tert -Butanol: A Cornerstone for High Performance Fluorine-19 Magnetic Resonance Imaging. *Chem. Commun.* **2021**, *57* (63), 7743−7757.
(11) Jiang, Z.-X.; Yu, Y. The Design and Synthesis of Highly Branched and Spherically Symmetric Fluorinated Macrocyclic Chelators. *Synthesis (Stuttg)* **2008**, *2008* (2), 215−220.
(12) Tirotta, I.; Mastropietro, A.; Cordiglieri, C.; Gazzera, L.; Baggi, F.; Baselli, G.; Bruzzone, M. G.; Zucca, I.; Cavallo, G.; Terraneo, G.; Baldelli Bombelli, F.; Metrangolo, P.; Resnati, G. A Superfluorinated Molecular Probe for Highly Sensitive in Vivo 19 F-MRI. *J. Am. Chem. Soc.* **2014**, *136* (24), 8524−8527.
(13) Martinez Espinoza, M. I.; Sori, L.; Pizzi, A.; Terraneo, G.; Moggio, I.; Arias, E.; Pozzi, G.; Orlandi, S.; Dichiarante, V.; Metrangolo, P.; Cavazzini, M.; Baldelli Bombelli, F. BODIPY Dyes Bearing Multibranched Fluorinated Chains: Synthesis, Structural, and Spectroscopic Studies. *Chem.-Eur. J.* **2019**, *25* (38), 9078−9087.
(14) Rosati, M.; Acocella, A.; Pizzi, A.; Turtù, G.; Neri, G.; Demitri, N.; Nonappa; Raffaini, G.; Donnio, B.; Zerbetto, F.; Bombelli, F. B.; Cavallo, G.; Metrangolo, P. Janus-Type Dendrimers Based on Highly Branched Fluorinated Chains with Tunable Self-Assembly and 19 F Nuclear Magnetic Resonance Properties. *Macromolecules* **2022**, *55* (7), 2486−2496.
(15) Dichiarante, V.; Tirotta, I.; Catalano, L.; Terraneo, G.; Raffaini, G.; Chierotti, M. R.; Gobetto, R.; Baldelli Bombelli, F.; Metrangolo, P. Superfluorinated and NIR-Luminescent Gold Nanoclusters. *Chem. Commun.* **2017**, *53* (3), 621−624.
(16) Kawai, F. Microbial Degradation of Polyethers. *Appl. Microbiol. Biotechnol.* **2002**, *58* (1), 30−38.
(17) Schmidt, T. C.; Schirmer, M.; Weiß, H.; Haderlein, S. B. Microbial Degradation of Methyl Tert-Butyl Ether and Tert-Butyl Alcohol in the Subsurface. *J. Contam. Hydrol.* **2004**, *70* (3−4), 173−203.
(18) Dichiarante, V.; Martinez Espinoza, M. I.; Gazzera, L.; Vuckovac, M.; Latikka, M.; Cavallo, G.; Raffaini, G.; Oropesa-Nuñez, R.; Canale, C.; Dante, S.; Marras, S.; Carzino, R.; Prato, M.; Ras, R. H. A.; Metrangolo, P. A Short-Chain Multibranched Perfluoroalkyl Thiol for More Sustainable Hydrophobic Coatings. *ACS Sustain. Chem. Eng.* **2018**, *6* (8), 9734−9743.
(19) Jacoby, C.; Temme, S.; Mayenfels, F.; Benoit, N.; Krafft, M. P.; Schubert, R.; Schrader, J.; Flögel, U. Probing Different Perfluorocarbons for in Vivo Inflammation Imaging by 19 F MRI: Image Reconstruction, Biological Half-Lives and Sensitivity. *NMR Biomed.* **2014**, *27* (3), 261−271.
(20) Chirizzi, C.; De Battista, D.; Tirotta, I.; Metrangolo, P.; Comi, G.; Bombelli, F. B.; Chaabane, L. Multispectral MRI with Dual Fluorinated Probes to Track Mononuclear Cell Activity in Mice. *Radiology* **2019**, *291* (2), 351−357.
(21) Ayaz, N.; Dichiarante, V.; Pigliacelli, C.; Repossi, J.; Gazzera, L.; Boreggio, M.; Maiolo, D.; Chirizzi, C.; Bergamaschi, G.; Chaabane, L.; Fasoli, E.; Metrangolo, P.; Baldelli Bombelli, F. Hydrophobin-Coated Solid Fluorinated Nanoparticles for 19 F-MRI. *Adv. Mater. Interfaces* **2022**, *9* (18), 2101677.
(22) Jamgotchian, L.; Vaillant, S.; Selingue, E.; Doerflinger, A.; Belime, A.; Vandamme, M.; Pinna, G.; Ling, W. L.; Gravel, E.; Mériaux, S.; Doris, E. Tumor-Targeted Superfluorinated Micellar Probe for Sensitive in Vivo 19 F-MRI. *Nanoscale* **2021**, *13* (4), 2373−2377.
(23) Koshkina, O.; White, P. B.; Staal, A. H. J.; Schweins, R.; Swider, E.; Tirotta, I.; Tinnemans, P.; Fokkink, R.; Veltien, A.; van Riessen, N. K.; van Eck, E. R. H.; Heerschap, A.; Metrangolo, P.; Baldelli Bombelli, F.; Srinivas, M. Nanoparticles for "Two Color" 19F Magnetic Resonance Imaging: Towards Combined Imaging of Biodistribution and Degradation. *J. Colloid Interface Sci.* **2020**, *565*, 278−287.
(24) Schöttler, S.; Becker, G.; Winzen, S.; Steinbach, T.; Mohr, K.; Landfester, K.; Mailänder, V.; Wurm, F. R. Protein Adsorption Is Required for Stealth Effect of Poly(Ethylene Glycol)- and Poly-(Phosphoester)-Coated Nanocarriers. *Nat. Nanotechnol.* **2016**, *11* (4), 372−377.
(25) Estapé Senti, M.; de Jongh, C. A.; Dijkxhoorn, K.; Verhoef, J. J. F.; Szebeni, J.; Storm, G.; Hack, C. E.; Schiffelers, R. M.; Fens, M. H.; Boross, P. Anti-PEG Antibodies Compromise the Integrity of PEGylated Lipid-Based Nanoparticles via Complement. *J. Controlled Release* **2022**, *341*, 475−486.
(26) Zhang, P.; Sun, F.; Liu, S.; Jiang, S. Anti-PEG Antibodies in the Clinic: Current Issues and beyond PEGylation. *J. Controlled Release* **2016**, *244*, 184−193.
(27) Koshkina, O.; Westmeier, D.; Lang, T.; Bantz, C.; Hahlbrock, A.; Würth, C.; Resch-Genger, U.; Braun, U.; Thiermann, R.; Weise, C.; Eravci, M.; Mohr, B.; Schlaad, H.; Stauber, R. H.; Docter, D.; Bertin, A.; Maskos, M. Tuning the Surface of Nanoparticles: Impact of Poly(2-Ethyl-2-Oxazoline) on Protein Adsorption in Serum and Cellular Uptake. *Macromol. Biosci.* **2016**, *16* (9), 1287−1300.
(28) Friedl, J. D.; Nele, V.; De Rosa, G.; Bernkop-Schnürch, A. Bioinert, Stealth or Interactive: How Surface Chemistry of Nanocarriers Determines Their Fate In Vivo. *Adv. Funct. Mater.* **2021**, *31* (34), 2103347.
(29) Gazzera, L.; Corti, C.; Pirrie, L.; Paananen, A.; Monfredini, A.; Cavallo, G.; Bettini, S.; Giancane, G.; Valli, L.; Linder, M. B.; Resnati, G.; Milani, R.; Metrangolo, P. Hydrophobin as a Nanolayer Primer That Enables the Fluorinated Coating of Poorly Reactive Polymer Surfaces. *Adv. Mater. Interfaces* **2015**, *2* (14), 1500170.
(30) Maiolo, D.; Pigliacelli, C.; Sánchez Moreno, P.; Violatto, M. B.; Talamini, L.; Tirotta, I.; Piccirillo, R.; Zucchetti, M.; Morosi, L.; Frapolli, R.; Candiani, G.; Bigini, P.; Metrangolo, P.; Baldelli Bombelli, F. Bioreducible Hydrophobin-Stabilized Supraparticles for Selective Intracellular Release. *ACS Nano* **2017**, *11* (9), 9413−9423.
(31) Pigliacelli, C.; Maiolo, D.; Nonappa; Haataja, J. S.; Amenitsch, H.; Michelet, C.; Sánchez Moreno, P.; Tirotta, I.; Metrangolo, P.; Baldelli Bombelli, F. Efficient Encapsulation of Fluorinated Drugs in the Confined Space of Water-Dispersible Fluorous Supraparticles. *Angew. Chemie Int. Ed.* **2017**, *56* (51), 16186−16190.
(32) Milani, R.; Monogioudi, E.; Baldrighi, M.; Cavallo, G.; Arima, V.; Marra, L.; Zizzari, A.; Rinaldi, R.; Linder, M.; Resnati, G.; Metrangolo, P. Hydrophobin: Fluorosurfactant-like Properties without Fluorine. *Soft Matter* **2013**, *9* (28), 6505.
(33) Hoogendijk, E.; Swider, E.; Staal, A. H. J.; White, P. B.; van Riessen, N. K.; Glaßer, G.; Lieberwirth, I.; Musyanovych, A.; Serra, C. A.; Srinivas, M.; Koshkina, O. Continuous-Flow Production of Perfluorocarbon-Loaded Polymeric Nanoparticles: From the Bench to Clinic. *ACS Appl. Mater. Interfaces* **2020**, *12* (44), 49335−49345.
(34) Koshkina, O.; Lajoinie, G.; Baldelli Bombelli, F.; Swider, E.; Cruz, L. J.; White, P. B.; Schweins, R.; Dolen, Y.; van Dinther, E. A. W.; van Riessen, N. K.; Rogers, S. E.; Fokkink, R.; Voets, I. K.; van Eck, E. R. H.; Heerschap, A.; Versluis, M.; de Korte, C. L.; Figdor, C. G.; de Vries, I. J. M.; Srinivas, M. Multicore Liquid Perfluorocarbon-Loaded Multimodal Nanoparticles for Stable Ultrasound and 19 F MRI Applied to In Vivo Cell Tracking. *Adv. Funct. Mater.* **2019**, *29* (19), 1806485.
(35) Staal, A. H. J.; Becker, K.; Tagit, O.; Koen van Riessen, N.; Koshkina, O.; Veltien, A.; Bouvain, P.; Cortenbach, K. R. G.; Scheenen, T.; Flögel, U.; Temme, S.; Srinivas, M. In Vivo Clearance of 19F MRI Imaging Nanocarriers Is Strongly Influenced by Nanoparticle Ultrastructure. *Biomaterials* **2020**, *261*, 120307.
(36) Nuhn, L.; Van Herck, S.; Best, A.; Deswarte, K.; Kokkinopoulou, M.; Lieberwirth, I.; Koynov, K.; Lambrecht, B. N.; De Geest, B. G. FRET Monitoring of Intracellular Ketal Hydrolysis in Synthetic Nanoparticles. *Angew. Chemie Int. Ed.* **2018**, *57* (33), 10760−10764.
(37) Chirizzi, C.; Morasso, C.; Caldarone, A. A.; Tommasini, M.; Corsi, F.; Chaabane, L.; Vanna, R.; Bombelli, F. B.; Metrangolo, P. A Bioorthogonal Probe for Multiscale Imaging by 19 F-MRI and Raman

https://doi.org/10.1021/accountsmr.2c00203
Acc. Mater. Res. XXXX, XXX, XXX−XXX

Microscopy: From Whole Body to Single Cells. *J. Am. Chem. Soc.* **2021**, *143* (31), 12253−12260.
(38) Jiang, Z.-X.; Yu, Y. B. The Design and Synthesis of Highly Branched and Spherically Symmetric Fluorinated Oils and Amphiles. *Tetrahedron* **2007**, *63* (19), 3982−3988.
(39) Jiang, Z.-X.; Liu, X.; Jeong, E.-K.; Yu, Y. B. Symmetry-Guided Design and Fluorous Synthesis of a Stable and Rapidly Excreted Imaging Tracer for 19 F MRI. *Angew. Chemie Int. Ed.* **2009**, *48* (26), 4755−4758.
(40) Jiang, Z.-X.; Yu, Y. B. Fluorous Mixture Synthesis of Asymmetric Dendrimers. *J. Org. Chem.* **2010**, *75* (6), 2044−2049.
(41) Yue, X.; Taraban, M. B.; Hyland, L. L.; Yu, Y. B. Avoiding Steric Congestion in Dendrimer Growth through Proportionate Branching: A Twist on Da Vinci's Rule of Tree Branching. *J. Org. Chem.* **2012**, *77* (20), 8879−8887.
(42) Lv, J.; Wang, H.; Rong, G.; Cheng, Y. Fluorination Promotes the Cytosolic Delivery of Genes, Proteins, and Peptides. *Acc. Chem. Res.* **2022**, *55* (5), 722−733.
(43) Shi, H.; Lai, B.; Chen, S.; Zhou, X.; Nie, J.; Ma, J.-A. Facile Synthesis of Novel Perfluorocarbon-Modulated 4-Anilinoquinazoline Analogues. *Chin. J. Chem.* **2017**, *35* (11), 1693−1700.
(44) Waiczies, S.; Millward, J. M.; Starke, L.; Delgado, P. R.; Huelnhagen, T.; Prinz, C.; Marek, D.; Wecker, Di.; Wissmann, R.; Koch, S. P.; Boehm-Sturm, P.; Waiczies, H.; Niendorf, T.; Pohlmann, A. Enhanced Fluorine-19 MRI Sensitivity Using a Cryogenic Radiofrequency Probe: Technical Developments and Ex Vivo Demonstration in a Mouse Model of Neuroinflammation. *Sci. Rep.* **2017**, *7* (1), 9808.
(45) Zhang, Y.; Bo, S.; Feng, T.; Qin, X.; Wan, Y.; Jiang, S.; Li, C.; Lin, J.; Wang, T.; Zhou, X.; Jiang, Z.; Huang, P. A Versatile Theranostic Nanoemulsion for Architecture-Dependent Multimodal Imaging and Dually Augmented Photodynamic Therapy. *Adv. Mater.* **2019**, *31* (21), 1806444.
(46) Huynh, A. M.; Müller, A.; Kessler, S. M.; Henrikus, S.; Hoffmann, C.; Kiemer, A. K.; Bücker, A.; Jung, G. Small BODIPY Probes for Combined Dual 19 F MRI and Fluorescence Imaging. *ChemMedChem.* **2016**, *11* (14), 1568−1575.
(47) Wang, M.; Liu, H.; Li, L.; Cheng, Y. A Fluorinated Dendrimer Achieves Excellent Gene Transfection Efficacy at Extremely Low Nitrogen to Phosphorus Ratios. *Nat. Commun.* **2014**, *5* (1), 3053.
(48) Decato, S.; Bemis, T.; Madsen, E.; Mecozzi, S. Synthesis and Characterization of Perfluoro-Tert-Butyl Semifluorinated Amphiphilic Polymers and Their Potential Application in Hydrophobic Drug Delivery. *Polym. Chem.* **2014**, *5* (22), 6461−6471.
(49) Taraban, M. B.; Deredge, D. J.; Smith, M. E.; Briggs, K. T.; Feng, Y.; Li, Y.; Jiang, Z.-X.; Wintrode, P. L.; Yu, Y. B. Conformational Transition of a Non-Associative Fluorinated Amphiphile in Aqueous Solution. II. Conformational Transition vs. Supramolecular Assembly. *RSC Adv.* **2019**, *9* (4), 1956−1966.
(50) Singh, A. K.; Schade, B.; Rosati, M.; Rashmi, R.; Dichiarante, V.; Cavallo, G.; Metrangolo, P.; Haag, R. Synthesis and Linker-Controlled Self-Assembly of Dendritic Amphiphiles with Branched Fluorinated Tails. *Macromol. Biosci.* **2022**, *22*, 2200108.
(51) Neri, G.; Mion, G.; Pizzi, A.; Celentano, W.; Chaabane, L.; Chierotti, M. R.; Gobetto, R.; Li, M.; Messa, P.; De Campo, F.; Cellesi, F.; Metrangolo, P.; Baldelli Bombelli, F. Fluorinated PLGA Nanoparticles for Enhanced Drug Encapsulation and 19 F NMR Detection. *Chem.-Eur. J.* **2020**, *26* (44), 10057−10063.
(52) Meng, B.; Grage, S. L.; Babii, O.; Takamiya, M.; MacKinnon, N.; Schober, T.; Hutskalov, I.; Nassar, O.; Afonin, S.; Koniev, S.; Komarov, I. V.; Korvink, J. G.; Strähle, U.; Ulrich, A. S. Highly Fluorinated Peptide Probes with Enhanced In Vivo Stability for 19 F-MRI. *Small* **2022**, *18*, 2107308.
(53) Feng, Z.; Li, Q.; Wang, W.; Ni, Q.; Wang, Y.; Song, H.; Zhang, C.; Kong, D.; Liang, X.-J.; Huang, P. Superhydrophilic Fluorinated Polymer and Nanogel for High-Performance 19F Magnetic Resonance Imaging. *Biomaterials* **2020**, *256*, 120184.
(54) Jahromi, A. H.; Wang, C.; Adams, S. R.; Zhu, W.; Narsinh, K.; Xu, H.; Gray, D. L.; Tsien, R. Y.; Ahrens, E. T. Fluorous-Soluble Metal Chelate for Sensitive Fluorine-19 Magnetic Resonance Imaging Nanoemulsion Probes. *ACS Nano* **2019**, *13* (1), 143−151.
(55) Lin, H.; Tang, X.; Li, A.; Gao, J. Activatable 19 F MRI Nanoprobes for Visualization of Biological Targets in Living Subjects. *Adv. Mater.* **2021**, *33* (50), 2005657.
(56) Pigliacelli, C.; Acocella, A.; Díez, I.; Moretti, L.; Dichiarante, V.; Demitri, N.; Jiang, H.; Maiuri, M.; Ras, R. H. A.; Bombelli, F. B.; Cerullo, G.; Zerbetto, F.; Metrangolo, P.; Terraneo, G. High-Resolution Crystal Structure of a 20 KDa Superfluorinated Gold Nanocluster. *Nat. Commun.* **2022**, *13* (1), 2607.
(57) Arango, J. M.; Padro, D.; Blanco, J.; Lopez-Fernandez, S.; Castellnou, P.; Villa-Valverde, P.; Ruiz-Cabello, J.; Martin, A.; Carril, M. Fluorine Labeling of Nanoparticles and In Vivo 19 F Magnetic Resonance Imaging. *ACS Appl. Mater. Interfaces* **2021**, *13* (11), 12941−12949.

https://doi.org/10.1021/accountsmr.2c00203
Acc. Mater. Res. XXXX, XXX, XXX−XXX